

Shear Piezoresistance Coefficient π_{44} of n-type Silicon

Yozo Kanda* and Kazunori Matsuda**

*Kojundo Chemical Laboratory Co. LTD

5-1-28 Chiyoda, Sakado, Saitama, 350-0284, Japan, ykanda@kojundo.co.jp

**Tokushima Bunri University at Kagawa

1314-1 Shido, Sanuki, Kagawa, 769-2193, Japan, kmatsuda@fe.bunri-u.ac.jp

ABSTRACT

Special attention should be paid when one wants to obtain the piezoresistance coefficients of n-type Si in an arbitrary temperature and carrier concentration. While the temperature and carrier concentration dependencies of the piezoresistance tensor components π_{11} and π_{12} are expressed by the piezoresistance factor, those of π_{44} are independent up to 10^{20} cm⁻³. Although concentration effective masses are affected by shear stress, the density-of-state effective mass does not change.

Keywords: n-Si, piezoresistance, MEMS, strain engineering, temperature and concentration dependencies

1 INTRODUCTION

Over half a century has passed since Smith reported the piezoresistance (PR) effect in germanium and silicon [1]. Recently, ULSI's world is entering into a new era of "strain engineering" in which PR plays an important role. The PR in silicon has been widely using in the frame work of micro electro mechanical system (MEMS).

A quarter of a century ago, one of the authors (Y.K.) pointed out the importance of the PR and provided the design data of the PR for both sensor engineers and integrated circuits engineering [2]. With technology advance, however, more precise data of PR are required.

Origin of the PR effect even in n-type Si was not always explained completely in spite of simpler band structure than that of p-type Si [3].

In the present paper, we recapitulate the origin of PR briefly. Stress-dependence of effective masses, and temperature and concentration dependence of the PR coefficient are discussed. Nonlinearity of the PR is also touched on. Finally, we give a complete understanding of the PR in n-Si.

2 ORIGIN OF π_{44} AND π_{12}

The PR effect is a forth-rank tensor which has three components π_{11} (longitudinal), π_{12} (transverse) and π_{44} (shear) for a cubic crystal, such as Si and Ge. According to Herring's theory [4], we obtain the tensor components. The conduction band consists of six valleys. Energy surfaces of

those valleys are ellipsoids of revolution aligned of with the principal crystal axes. If a uniaxial tension is applied along $\langle 100 \rangle$ the x-valleys move up and the y- and z-valleys move down. Electrons in the x-valleys transfer to the y- and z-valleys keeping total number of electrons constants. The relative change in resistivity along $\langle 100 \rangle$ and $\langle 010 \rangle$ give the PR tensor components π_{11} and π_{12} , respectively. Next, the longitudinal π_l ($i \parallel \langle 110 \rangle$) and the transverse π_t ($i \perp \langle 110 \rangle$) are considered under a uniaxial tension along $\langle 110 \rangle$.

$$\pi_{l\langle 110 \rangle} = 1/2(\pi_{11} + \pi_{12} + \pi_{44}) \quad (1)$$

$$\pi_{t\langle 110 \rangle} = 1/2(\pi_{11} + \pi_{12} - \pi_{44}) \quad (2)$$

$$\pi_{l\langle 110 \rangle} - \pi_{t\langle 110 \rangle} = \pi_{44} \quad (3)$$

In this case the six valleys don't move. Energy surfaces are ellipsoids of revolution and the six valleys as a whole look the same whether looked along $\langle 100 \rangle$ (longitudinal) or along $\langle 110 \rangle$ (transverse).

Therefore, the π_{44} vanishes. Theoretical expressions for these are,

$$\pi_{11} = (2\Xi_u/3k_B T)(s_{11} - s_{12})(1 - L)(1 + 2L) \quad (4)$$

$$\pi_{12} = -(\Xi_u/3k_B T)(s_{11} - s_{12})(1 - L)(1 + 2L) \quad (5)$$

$$\pi_{44} = 0 \quad (6)$$

where Ξ_u is the shear deformation potential, s_{ij} 's are the compliance constants, $L = m_l/m_t$, $m_l = 0.1963m$, $m_t = 0.9105m$. k_B is the Boltzmann constant and T is the absolute temperature.

3 EFFECTIVE MASS CHANGE

The observed π_{44} is in fact small compared with other components π_{11} and π_{12} but differs from zero beyond experimental error ($\pi_{44} = -13.6$, $\pi_{11} = -102.2$, $\pi_{12} = 53.4$ in 10^{-11} Pa⁻¹) [1]. We consider the effect of strain on the electron effective mass which has been hitherto neglected. The energy band diagram of Si is shown in Fig.1(a). The minima of conduction band, Δ_1 are located at 0.85 distance from Γ point to the zone boundary X point (close to X point). The conduction bands Δ_1 and Δ_2' touch at X point due to a special symmetry of the diamond structure. This degeneracy is removed by shear stress and the consequent

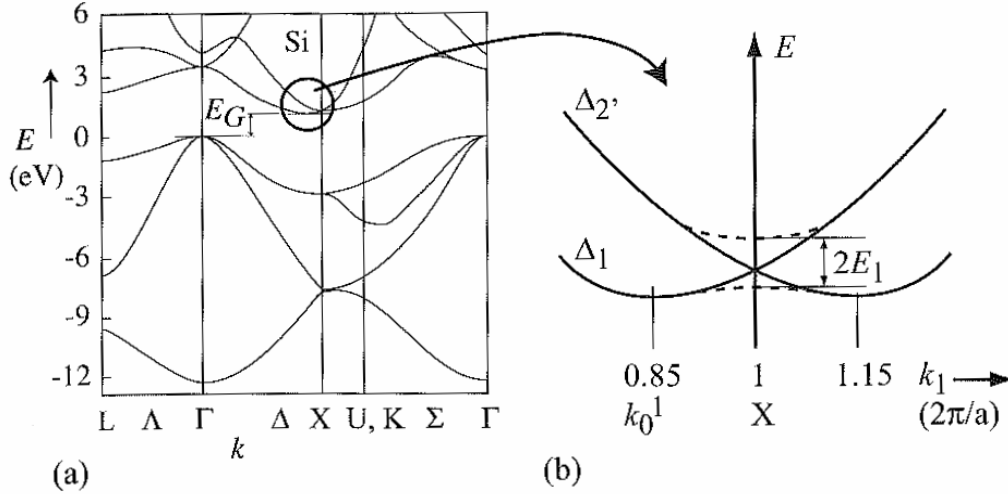


Fig. 1.(a) Energy band Diagram, (b) Degenerate conduction band Δ_1 and Δ_2 at point X and its lifting with a shear strain by an amount of $2E_1$ [5].

electron effective mass shifts of Δ_1 band due to strain mixing of the electron wave functions [5].

As shown in Fig.1 (b), the two bands splits by an amount $2E_1$. A shear stress destroys the rotational symmetry of the ellipsoidal valleys and induces large effective mass changes. We pay attention to the ellipsoid on the k_1 axis under shear stress e_{xy} . As shown in Fig.2, The energy surface is no longer an ellipsoid of revolution, but an ellipsoid with three different radii along its principal axes. In particular it gives different effective masses.

$$1/m_1(e) = 1/m_t + \alpha \cdot e_{23} \quad (7)$$

$$1/m_2(e) = 1/m_t - \alpha \cdot e_{23} \quad (8)$$

$$1/m_3(e) = 1/m_l \quad (9)$$

The effective masses of other valleys are not affected by shear strain e_{23} . Under a rather general assumption on the relaxation time τ , the electron conductivity in Si is given by

$$\sigma_0 = ne^2 \langle \tau \rangle / 3(1/m_l + 2/m_t) \quad (10)$$

where n is the electron concentration. The longitudinal and transverse conductivities are given under the same condition

$$\sigma_l = ne^2 \langle \tau \rangle / 3(1/m_l + 1/m_t + 1/m_1(e)) \quad (11)$$

$$\sigma_t = ne^2 \langle \tau \rangle / 3(1/m_l + 1/m_t + 1/m_2(e)) \quad (12)$$

Although conduction effective masses are affected by strain, the DOS masses remain unchanged,

$$m_1(e) \cdot m_2(e) \cdot m_3(e) = m_l m_t^2 \quad (13)$$

This fact was confirmed experimentally by the piezo capacitance effect [6].

4 ORIGIN OF π_{44}

From equations (7)- (12) we obtain

$$\begin{aligned} \frac{\sigma_l - \sigma_t}{\sigma_0} &= \frac{1/m_1(e) - 1/m_2(e)}{1/m_l + 2/m_t} = \frac{2\alpha \cdot e_{23}}{1/m_l + 2/m_t} \\ &= \frac{\alpha \cdot s_{44} \cdot T_{23}}{1/m_l + 2/m_t} \end{aligned} \quad (14)$$

On the other hand, from Eqs.(1)-(3) and $\sigma = 1/\rho$, we have [7],

$$\pi_{44} = \frac{-\alpha \cdot m_l \cdot s_{44}}{1 + 2L} \quad (15)$$

Since $\alpha = (86.8 \pm 5.0)/m$ [5] and $s_{44} = 1.248 \times 10^{-11} \text{ Pa}^{-1}$ the π_{44} is evaluated as $-9.4 \times 10^{-11} \text{ Pa}^{-1}$ which is of the same sign and magnitude with the experimental values mentioned earlier. A similar effect was detected in n-channel MOS transistors [8]. This origin is quite different from the stress induced inter-valley electron transfer which has long been believed to be the dominant source of PR in many-valley semiconductors [4]. The former Eq.(14) is temperature independent, while the latter Eqs. (4) and (5) are inversely proportional to absolute temperature.

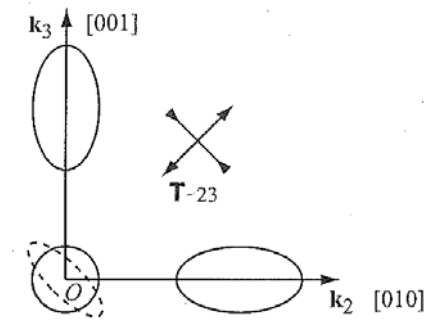


Fig.2 Schematic diagram of the $\langle 100 \rangle$ valley in k space under a shear stress T_{23} . Dashed line show the effect of stress.

5 CONCENTRATION AND TEMPERATURE DEPENDENCIES

Smith's data ($\pi_{11} = -102.2$, $\pi_{12} = 53.4$, $\pi_{44} = -13.6$ in unit of 10^{-11} Pa^{-1}) were taken at room temperature for low impurity concentration samples $\pi_{ij}(300\text{K})$ [1]. In general, the PR coefficients for arbitrary impurity concentration and at arbitrary temperature $\pi(N_D, N_A, T)$ have been expressed by using derivative of conductivity with respect to the reduced energy η [2,9].

$$\pi(N_D, N_A, T) = \text{PRF} \cdot \pi(300\text{K}) \quad (16)$$

$$\text{PRF} = \frac{300}{T} \frac{1}{\sigma} \frac{d\sigma}{d\eta} \quad (17)$$

The conductivity of semiconductors is given by the relaxation approximation of Boltzmann transport theory, in which the reciprocal of total relaxation time is the sum of the reciprocal relaxation time for each process, i.e. phonon, ionized impurity, and neutral impurity scatterings. Although the neutral impurity scattering has a minor effect at room temperature, we pay attention to short channel nMOSFETs with halo (or pocket) in which carriers are highly compensated. The PRF depends on temperature and impurity concentration.

Equation (16) is valid for p-type material (π_{11} , π_{12} , π_{44}) and n-type π_{11} , and π_{12} but not for n-type π_{44} . As shown in Eqs. (4), (5), and (14), the π_{44} is distinct from π_{11} and π_{12} in temperature and also carrier concentration dependencies. Tufte and Stelzer [10] showed experimentally that the π_{44} is independent of carrier concentration up to 10^{20} cm^{-3} and logarithmically proportional to carrier concentration above 10^{20} cm^{-3} . Special attention should be paid in using n-type Si since ULSI's (CMOS) and MEMS are often made in n-type [110]:

$$\pi_{[110]}(N_D, N_A, T) = (\text{PRF}(\pi_{11} + \pi_{12}) + \pi_{44}) / 2 \quad (18)$$

$$N_D \leq 10^{20} \text{ cm}^{-3}$$

$$\pi_{[110]}(N_D, N_A, T) = (\text{PRF}(\pi_{11} + \pi_{12}) + \pi_{44}) / 2 \quad (19)$$

$$N_D > 10^{20} \text{ cm}^{-3}$$

Although Eqs. (18) and (19) are for longitudinal PR, these become for transverse PR by replacing sign of π_{44} . In general, the PR tensor for n-type Si is desirable to be written as follow.

$$\pi = \begin{pmatrix} \pi_{11}P & \pi_{12}P & \pi_{12}P & 0 & 0 & 0 \\ \pi_{12}P & \pi_{11}P & \pi_{12}P & 0 & 0 & 0 \\ \pi_{12}P & \pi_{12}P & \pi_{11}P & 0 & 0 & 0 \\ 0 & 0 & 0 & \pi_{44} & 0 & 0 \\ 0 & 0 & 0 & 0 & \pi_{44} & 0 \\ 0 & 0 & 0 & 0 & 0 & \pi_{44} \end{pmatrix} \quad (20)$$

This gives a universal PR tensor for n-type Si, here, $P = \text{PRF}$.

The phenomenon above 10^{20} cm^{-3} of π_{44} is explained as follows; higher carrier concentration lowers the Fermi level due to the tail of the DOS.

The characteristics of π_{44} are so strange that π_{44} can be used as the tool to evaluate various softwares. We consider a four-terminal device such as Hall effect device in [100] n-Si whose current flow I , along $\langle 010 \rangle$. We measure a trasverse voltage V_{out} under shear stress T_{23} . The proportionality constant defines π_{44} .

$$V_{out} = \pi_{44} \cdot I \cdot T_{23} \quad (21)$$

6 NONLINEARITY

Recently, Chen and MacDonald measured the nonlinearity of [110] PR in n-Si above 10^{20} cm^{-3} [11]. This includes the effect of the band-tail [12]. On the other hand we did that below 10^{20} cm^{-3} [13]. This does not include the effect of the band-tail. We can imagine difference between them from Eqs. (18) and (19). Moreover, there is salient difference between the DOS below 10^{20} cm^{-3} (solid line) and that above 10^{20} cm^{-3} (dashed line) as shown in Fig. 3. It is obvious that the DOS with or without the band-tail affects the nonlinearity of the PR. This superposes on the above Eqs. (18) and (19). As the result, we give a complete understanding of the PR in n-Si above the hopping conduction temperature range.

Until now we have discussed on the piezoresistance effect of n-Si. These results and concept, however, are applicable to the piezo-Hall effect of n-type silicon [14,15].

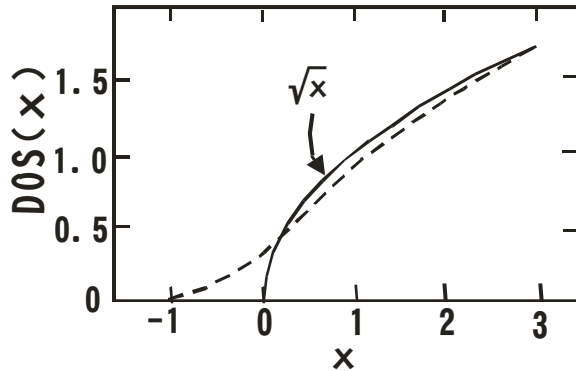


Fig.3 Dependence of DOS on energy: X is the reduced energy, solid line shows the DOS with the band-tail, dashed line shows DOS without the band-tail [12].

7 CONCLUSIONS

We gave the stress dependent conduction effective masses and the stress independent density-of-state effective mass. It was clarified that the π_{44} is distinct from π_{11} and π_{12} in temperature and carrier concentration dependencies. The former is independent of temperature while the latter is inversely proportional to absolute temperature. The former is independent of carrier concentration while the latter depend on carrier concentration through PRF. The universal PR

tensor was shown. It was suggested that the band-tail effect is taken into account to explain the PR at higher carrier concentration.

Finally, we give a complete understanding of the PR in n-type silicon.

ACKNOWLEDGEMENTS

This work was partially supported by the Grant-in-Aid for Scientific Research No.16510099 from JSPS.

REFERENCES

- [1] C. S. Smith, Phys. Rev. **94**, 42-49, 1954.
- [2] Y. Kanda, IEEE Trans. **ED-29**, 64-70, 1982.
- [3] Y. Kanda and K. Matsuda, ICPS-27 ed. by José Mrn éndez and Chris Van de Walle, AIP CP772, Melville, New York 2005, pp.79-80.
- [4] C. Herring and E. Vogt, Phys. Rev. **101**, 944-961, 1956.
- [5] J. C. Hensel, H. Hasegawa and M. Nakayama, Phys. Rev. **138**, 225-238, 1965.
- [6] K. Matsuda and Y. Kanda, Appl. Phys. Lett. **83**, 4353, 2003.
- [7] Y. Kanda and K. Suzuki, Phys. Rev. B **43**, 6754-6756, 1991.
- [8] T. Maruyama, S. Zaima, Y. Koide, Y. Kanda and Y. Yasuda, J. Appl. Phys. **68**, 5687-5691, 1990.
- [9] K. Matsuda and Y. Kanda, Proc. 2001 Int'l Cond. On MSM, Hilton Head Island, SC, USA, March 19-21, 2001, 346-349.
- [10] O. N. Tufte and E. L. Stelzer, Phys. Rev. **133**, A1705-A1716, 1964.
- [11] J. M. Chen and N. C. MacDonald, Rev. Scient. Instrum. **75**, 276-278, 2004.
- [12] M. I. Dykonov, A. L. Efros and D. L. Mitchell, Phys. Rev. **180**, 813-, 1969.
- [13] K. Matsuda, K. Suzuki, K. Yamamura and Y. Kanda, J. Appl. Phys. **73**, 1838-1847, 1993.
- [14] H. Hälgl, J. Appl. Phys. **64**, 276-282, 1988.
- [15] Y. Kanda and K. Suzuki, ICPS-22, Proceeding, Vancouver, Canada, 89-92, 1994.